TRANSACTIONS OF THE INSTITUTE OF FLUID-FLOW MACHINERY

No. 135, 2017, 73–85

Krzysztof Tesch* and Katarzyna Kaczorowska

Minimum drag shape bodies moving in inviscid fluid – revisited

Gdańsk University of Technology Fluid Mechanics Department
G. Narutowicza 11/12 80-233 Gdańsk

Abstract

This paper presents the classic approach to minimum drag shape body problem, moving at hypersonic speeds, leading to famous power law shapes with value of the exponent of $\frac{3}{4}$. Two- and three-dimensional cases are considered. Furthermore, an exact pseudo solution is given and its uselessness is discussed. Two new solutions are introduced, namely an approximate solution due to form of the functional and solution by means of optimisation of a Bézier curve. The former transforms the variational problem to the classic problem of function optimisation by assuming certain class of functions, whereas the latter by means of discretised functional.

Keywords: Minimum drag; Variational calculus; Optimisation

Nomenclature

A	–	reference area
C	–	constant, crossover probability
c_d	–	drag coefficient
c_p	–	pressure coefficient
F	–	scale parameter

*Corresponding author. E-mail address: krzyte@pg.gda.pl

$\mathbf{g}$	–	global optimum
H	–	Heaviside step function
J	–	functional
$\mathbf{K}$	–	vector
L	–	curve
n	–	exponent
N	–	population size
$n_{\max}$	–	total number of iterartion
$\hat{\mathbf{n}}$	–	normal unit vector
p	–	pressure
R_x	–	drag force
$\mathbf{R}$	–	total force exerted on a body
S	–	body's surface
U	–	velocity magnitude
x, y, z	–	independent variables
$\mathbf{x}$, $\mathbf{y}$	–	points

Greek symbols

α	–	angle
ρ	–	density

Other symbols

(.)', (.)"	–	first and second derivative

1 Problem formulation

Figure 1 presents a moving object in steady, inviscid and incompressible fluid at a constant speed U. Resistance is considered only on the peripheral of a moving object. Two cases are considered here, namely two-dimensional and three-dimensional. The shape of the body is symmetrical with respect to the x-axis, while in the latter one deals with an axial-symmetry with respect to the same axis.

2 Fluid Resistance

2.1 Drag force

Drag force is the components, directed towards the body velocity, of the total force, $\mathbf{R}$, exerted on the moving body by the fluid. Formally, the total force is defined by means of a surface integral of stress vector over a considered body's surface, S. In the absence of viscous (tangential) stresses this can be expressed

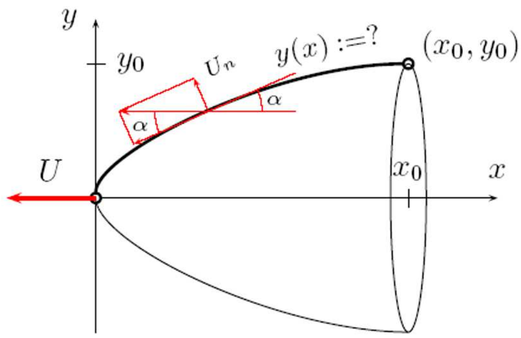

Figure 1: Body moving at hypersonic speeds.

by means of the normal stresses contribution [10]

$$\mathbf{R} = -\iint_S (p - p_\infty)\hat{\mathbf{n}}\,\mathrm{d}S \,, \tag{1}$$

where p_∞ is the free stream pressure.

For further consideration it is necessary to specify a unit normal vector $\hat{\mathbf{n}}$ to the surface S. If the surface S is given explicitly $S := \{(x, y, z)|z = f(x, y)\}$ or implicitly $S := \{(x, y, z)|F(x, y, z) := f(x, y) - z = 0\}$, the unit normal vector is

$$\hat{\mathbf{n}} = -\frac{\nabla F}{|\nabla F|} = \frac{(-z_x, -z_y, 1)}{\sqrt{1 + z_x^2 + z_y^2}} \,, \tag{2}$$

where the subscripts x and y denotes derivative respect to x- and y-axis, respectively. The above formula takes simpler form for both: two-dimensional and three-dimensional axisymmetric case

$$\hat{\mathbf{n}} = \frac{(-y', 1)}{\sqrt{1 + y'^2}} \,, \tag{3}$$

where the unit normal vector $\hat{\mathbf{n}}$ applies to the curve L given by $L := \{(x, y)|y = f(x)\}$ or $L := \{(x, y)|F(x, y) := f(x) - y = 0\}$, and symbol prim (') refers derivative respect to x-axis.

2.2 Pressure coefficients and its approximation

In order to determine drag force it is necessary to know the distribution of pressure difference $p - p_\infty$. The pressure may be determined when, for instance, the pressure coefficient distribution is known

$$c_p := \frac{p - p_\infty}{\frac{1}{2}\rho U_\infty^2} \,, \tag{4}$$

where U_∞ is the free stream velocity. The Newtonian approximation for the distribution of pressure coefficient is given by [1, 2, 4]

$$c_p = 2\sin^2\alpha \,, \tag{5}$$

where α denotes the angle between free stream velocity and tangent to body surface and together with definition (4) yields $p - p_\infty = \rho U_\infty^2 \sin^2\alpha$. This makes it possible to determine the optimal shape of a body moving in inviscid fluid in the sense of minimum drag.

Historically, the first calculations of a minimum drag body was performed by Newton [7]. The assumption is that the body is moving at high speeds, corresponding to hypersonic air flows, so the inertia forces are large enough. Newton's law of resistance neglects viscous forces, resulting in the local resisting pressure being proportional to the square of the free-stream velocity [2]. What is more, at hypersonic speeds oblique shock waves resembles flows assumed by Newton for the free-stream Mach number larger then 1 [2]. Provided that the curvature of the body is small, Eq. (5) is also valid for the pressure coefficient at the surface of the body. This, however, does not have to be true when the curvature of the body is large as the centrifugal forces between the shock and the surface may play important role [2]. Experimental results [1, 2, 5] indicate good agreement with theoretical prediction based on the pressure coefficient Eq. (5).

3 Two-dimensional problem

In the case of two-dimensional flows Eq. (1) is reduced to the following form:

$$\mathbf{R} = -\int_L (p - p_\infty)\hat{\mathbf{n}}\,\mathrm{d}L = -\rho U_\infty^2 \int_L \hat{\mathbf{n}}\sin^2\alpha\,\mathrm{d}L \,, \tag{6}$$

where the curve L starts from the point $(0,0)$ and ends at (x_0, y_0), see Fig. 1. From the same figure arises another geometrical relation, namely

$$\sin\alpha = \frac{\mathrm{d}y}{\sqrt{\mathrm{d}x^2 + \mathrm{d}y^2}} = \frac{y'}{\sqrt{1 + y'^2}}. \tag{7}$$

In order to convert curvilinear integral to single integral it is necessary to take advantage of arc differential $\mathrm{d}L = \sqrt{1 + y'^2}\,\mathrm{d}x$.

Drag force R_x comes directly from Eqs. (6), (3) and (7)

$$R_x = \rho U_\infty^2 \int_0^{x_0} \frac{y'^3}{1+y'^2}\,\mathrm{d}x \tag{8}$$

and can be interpreted as a certain functional J. The specific value of that functional depends on a curve of interest y. A constant value ρU_∞^2 is regarded here as a multiplier. This leads to the following form of this functional:

$$J[y] := \int_0^{x_0} \frac{y'^3}{1+y'^2}\,\mathrm{d}x = \int_0^{x_0} F(y,y')\,\mathrm{d}x \ . \tag{9}$$

The necessary condition for the optimum of the functional J results in the Euler equation [3]

$$F_y - \frac{\mathrm{d}}{\mathrm{d}x} F_{y'} = 0 \ , \tag{10}$$

where the subscripts y and y' refer to the function y describing minimum drag shape body and its the derivative, respectively. From the Euler equation (10), for the functional J we obtain an ordinary differential equation $y'y''(y'^2-3)=0$ (where the prime and double primes symbols are the first and second derivatives of y with respect to x-axis). There are four solutions to this equation. The first trivial solution $y = C_1$ (where C_1 is a constant) does not fulfil boundary conditions. For a specific case when $C_1 = 0$ and $y(x) = 0$ one obtains a solution characterised by zero drag. The second and third solutions, namely $y(x) = C_1 \pm \sqrt{3}x$, do not fulfil one boundary condition in general. For instance, if $y(0) = 0$ then $C_1 = 0$ and it is typically impossible to fulfil $y(x_0) = y_0$. The fourth solution $y(x) = C_1 + C_2 x$ satisfies both boundary conditions $y(0) = 0$, $y(x_0) = y_0$. Constants are determined to be $C_1 = 0$, $C_2 = y_0 x_0^{-1}$. This results in the following solution:

$$\frac{y}{y_0} = \frac{x}{x_0} \ . \tag{11}$$

Introducing dimensionless variables $x^+ = x\,x_0^{-1}$ and $y^+ = y\,y_0^{-1}$ we have somewhat simpler form $y^+ = x^+$. The above solutions is shown in Fig. 2. It is simply a straight line. Furthermore, an isosceles triangle is a two-dimensional body of a minimum drag.

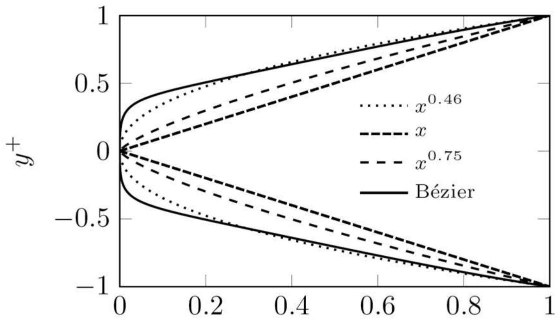

Figure 2: Optimal shapes.

4 Three-dimensional problem

4.1 Functional and Euler equation

In the case of two-dimensional surfaces S of revolutions Eq. (1) is reduced to the following form:

$$\mathbf{R} = -2\pi \int_L (p - p_\infty)\hat{\mathbf{n}} y \, \mathrm{d}L \, , \tag{12}$$

where the curve L is peripheral of surface S. Equation (12) is valid for axisymmetric problems. This results in different drag force equation in comparison with Eq. (8)

$$R_x := 2\pi\rho U_\infty^2 \int_0^{x_0} \frac{y'^3 y}{1+y'^2} \, \mathrm{d}x. \tag{13}$$

Neglecting constant multiplier $2\pi\rho U_\infty^2$ makes it now possible to express the functional J as

$$J[y] = \int_0^{x_0} \frac{y'^3 y}{1+y'^2} \, \mathrm{d}x \, . \tag{14}$$

Following the same line of reasoning we have the necessary condition for the optimum of the above functional. This results in the same Euler equation (10). This time, however, we obtain slightly more complicated ordinary differential equation

$$y' \left(y \, y'' \left(y'^2 - 3 \right) - y'^2 - y'^4 \right) = 0 \, . \tag{15}$$

This is an obvious consequence of a more complex form of a functional J. Solution to this equation has to fulfil the same boundary conditions as previously $y(0) = 0$, and $y(x_0) = y_0$.

4.2 Exact pseudo solution

A solution to nonlinear Eq. (15) may not be unique. It can, however, be integrated once setting simultaneously $y' = u(y)$ and $y'' = u'u$. This leads to another nonlinear equation $C_1 y\, y'^3 = (1+y'^2)^2$ this time of the first order. This equation can be classified as Lagrange equation and its parametric solution is

$$x(p) = \frac{1}{C_1}\left(\frac{3}{4p^4} + \frac{1}{p^2}\ln p + C_2\right), \tag{16a}$$

$$y(p) = \frac{\left(1+p^2\right)^2}{C_1 p^3}, \tag{16b}$$

where $p = y'$ is a parameter and derivative at the same time. It can be easily demonstrated keeping in mind that $\frac{\mathrm{d}y}{\mathrm{d}x} = \frac{\mathrm{d}y}{\mathrm{d}p}/\frac{\mathrm{d}x}{\mathrm{d}p} = p$. Unknown constant in Eq. (16) should satisfy boundary conditions. Solution (16) is of no practical value. This is because of nonlinear and non-unique character of Eq. (15). It possible to find the optimal solution only within the range of $x^+ \in [0.1, 1]$. Consequently, it is impossible to find the most interesting part of the solution around $x^+ \approx 0$.

4.3 Approximate solution due to the functional

The differential equation for the functional (15) has a complicated form. This means that it is extremely difficult to give an explicit solution. The classic approach to this problem is to simplify the form of a functional (14). It is assumed that $y'^2 \ll 1$ and hence $y'^2 + 1 \approx 1$. This assumption is not true when $x^+ \approx 0$ where one would expect $y'(x) \to \infty$ as $x \to 0^+$. This is because of smoothness of the axisymmetric solution. However, far from the point of stagnation the discussed simplification is justified. If so, then the form of functional (14) can be simplified

$$J[y] = \int_0^{x_0} y'^3 y \,\mathrm{d}x\,. \tag{17}$$

The necessary condition for the optimum of the above functional results in simpler Euler equation form: $y'(y'^2 + 3y\,y'') = 0$. There are two solutions to this equation. The first trivial solution $y = C_1$ does not fulfil boundary conditions. The second solution is $y(x) = C_2(4x - 3C_1)^{\frac{3}{4}}$. Applying boundary conditions $y(0) = 0$, and $y(x_0) = y_0$ we have

$$\frac{y}{y_0} = \left(\frac{x}{x_0}\right)^{\frac{3}{4}}. \tag{18}$$

The same in dimensionless variables yields $y^+ = (x^+)^{\frac{3}{4}}$. Solution of (18) has the form of a parabola and it is shown in Fig. 2.

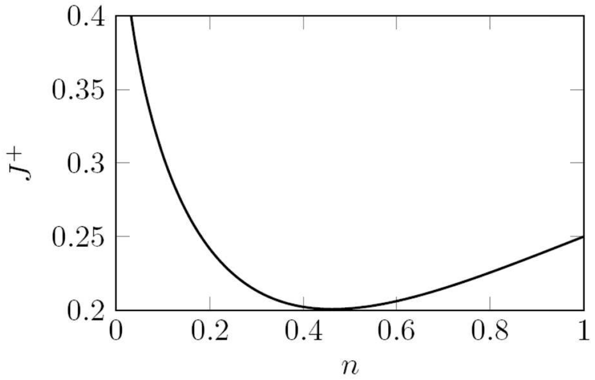

Figure 3: J^+ values as a function of the exponent n.

4.4 Approximate solution due to form of the function

It can be easily verified that following curve $y^+ = (x^+)^{\frac{1}{2}}$ gives even smaller value of the original functional (14) in comparison with $y^+ = (x^+)^{\frac{3}{4}}$ that minimises functional (17). This suggest that instead of simplified version of functional (14) one can consider certain class of functions. The natural candidate is

$$y^+ = \left(x^+\right)^n \ . \tag{19}$$

The unknown exponent n should be $n \in]0, +\infty[$. In spite of appearances, this is a fairly wide range of solutions, which can take the form of from a thin picket to almost a tube. The class of functions (19) satisfies boundary conditions in dimensionless form $y^+(0) = 0$, and $y^+(1) = 1$.

Known form of the function (19) allows to transform the variational problem to the classic problem of function optimisation. One looks for the optimal value of the exponent n. This method is somewhat similar to the Ritz method. Its approximate nature is in the fact that the family of assumed function (19) does not have to incorporate the exact solution of a functional (14). Functional (14) now takes the following form:

$$J^+ := \int_0^1 \frac{n^3 (x^+)^{4n-3}}{1 + n^2 (x^+)^{2n-2}} \, \mathrm{d}x^+ \tag{20}$$

and can be integrated only numerically. Figures 3 presents values of functional J^+ as a function of exponent n according to Eq. (20). It is now apparent that exponent $\frac{3}{4}$, being an optimal solution of simplified functional (17), is not the best solution when it comes to original functional (14). The optimal exponent within the class of functions (19) is $n \approx 0.46$. This leads to the optimal parabola $y^+ = (x^+)^{0.46}$ shown in Fig. 2.

4.5 Approximate solution by means of optimisation of a Bézier curve

Another approach to minimisation of functional (14) is to discretise the variational problem by means of Bézier curves. This means that the original problem $f : \mathbb{C}^2_{[0;1]} \to \mathbb{R}$ is now reduced to single variable optimisation $f : \mathbb{R}^D \to \mathbb{R}$ where

$$\mathbb{C}^2_{[0;1]} := \left\{ f \mid \quad f, f', f'' : [0;1] \to \mathbb{R} \quad \text{are continuous} \right\} . \tag{21}$$

Figure 6 shows an example of Bézier curve described by means of five points. First and last point are fixed as well as the x coordinate of the second point. The former geometrical constrain is necessary in order to keep the surface of revolution smooth. The assumed geometrical constrains results in five independent variables, i.e., $D = 5$.

If the objective function to be minimised is $f : \mathbb{R}^D \to \mathbb{R}$ then the constrained optimisation problem is

$$\min_{\mathbf{x} \in \Omega} f(\mathbf{x}) = f_0 , \tag{22}$$

where a D dimensional point is $\mathbf{x} = (x_1, x_2, \ldots, x_D)$. The objective function is subjected to box constrains

$$\Omega := \left\{ \mathbf{x} \in \mathbb{R}^D : L_i \le x_i \le U_i \right\} . \tag{23}$$

The argument $\mathbf{g}$ of the global minimum value of the objective function f is defined as

$$\mathbf{g} = \arg \min_{\mathbf{x} \in \Omega} f(\mathbf{x}) , \tag{24}$$

so that $f_0 = f(\mathbf{g})$. If $\Omega = \mathbb{R}^D$ one deals with unconstrained optimisation.

4.5.1 Optimisation algorithm

Differential evolution (DE) [9] is the state of the art global optimisation algorithms. It can be classified as biologically-inspired metaheuristic or multipoint, derivative free algorithm. DE may be regarded as an extension of genetic algorithms [6]. Mutation and binomial crossover are performed by means of the following rule:

$$\mathbf{y}_i = \mathbf{K} \circ (\mathbf{x}_a^n + F(\mathbf{x}_b^n - \mathbf{x}_c^n)) + (\mathbf{1} - \mathbf{K}) \circ \mathbf{x}_i^n , \tag{25}$$

Input: C, F, N, n_{max}, $\mathbf{L}$, $\mathbf{U}$
Output: $\mathbf{g}$
for $i := 0$ **to** $N-1$ **do**
  $\mathbf{x}_i := \mathbf{L} + (\mathbf{U} - \mathbf{L}) \circ \boldsymbol{\mathcal{U}}(0,1)$;
$\mathbf{g} := \arg\min_{\mathbf{x}_i} f(\mathbf{x}_i)$;
for $n := 1$ **to** $n_{max} - 1$ **do**
  for $i := 0$ **to** $N-1$ **do**
    $\mathbf{K} := \mathrm{H}\left(C - \boldsymbol{\mathcal{U}}(0,1)\right)$;
    $K_{\mathcal{U}\{0,D-1\}} := 1$;
    $\mathbf{a} := \mathrm{RandomPermutation}(\{0,\ldots,N-1\} \setminus \{i\})$;
    $\mathbf{y}_i := \mathbf{K} \circ \left(\mathbf{x}_{a_3} + F\left(\mathbf{x}_{a_1} - \mathbf{x}_{a_2}\right)\right) + (\mathbf{1} - \mathbf{K}) \circ \mathbf{x}_i$;
  for $i := 0$ **to** $N-1$ **do**
    $\mathbf{x}_i := \arg\min\left\{f(\mathbf{x}_i), f(\mathbf{y}_i)\right\}$;
    $\mathbf{g} := \arg\min\left\{f(\mathbf{g}), f(\mathbf{y}_i)\right\}$;

Figure 4: Differential evolution pseudocode.

where the vector $\mathbf{K}$ is defined as

$$\mathbf{K} = \mathrm{H}\left(C - \boldsymbol{\mathcal{U}}(0,1)\right) \ . \tag{26}$$

In the above F is the scale factor, C stands for crossover probability. Lower and upper domain constraints are denoted as $\mathbf{L}$ and $\mathbf{U}$ respectively. The subscripts a, b and c refer to three different individuals or the so-called candidate solutions among N vectors. Finally, the number of iterations is denoted as n_{max}. Selection is carried out by means of

$$\mathbf{x}_i^{n+1} = \begin{cases} \mathbf{y}_i & \text{if } f(\mathbf{y}_i) < f(\mathbf{x}_i^n), \\ \mathbf{x}_i^n & \text{otherwise.} \end{cases} \tag{27}$$

The two most popular variants of DE are listed below, namely

- DE/Rand/1/Bin

$$\mathbf{y}_i = \mathbf{x}_a^n + F\left(\mathbf{x}_b^n - \mathbf{x}_c^n\right), \tag{28}$$

- DE/Best/1/Bin

$$\mathbf{y}_i = \mathbf{g}^n + F\left(\mathbf{x}_b^n - \mathbf{x}_c^n\right). \tag{29}$$

The complete pseudocode of DE is shown in Fig. 4.

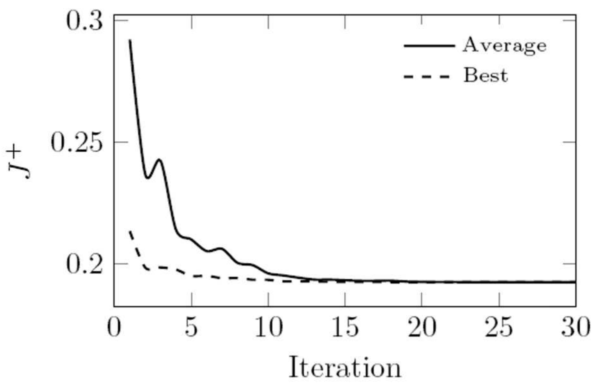

Figure 5: Convergence

4.5.2 Results

Uniform random initialisation within the search space with random seed based on time was considered. The algorithms stopped when the number of generations $n_{\max} = 30$ was reached. The total number of solution per generation (population size) was $N = 20$. The scale parameter F of DE and the crossover probability C are listed in Tab. 1 together with other optimisation parameters such as lower $\mathbf{L}$ and upper $\mathbf{U}$ box constrains.

Table 1: Basic parameters of an algorithm.

Symbol	Value
D	5
N	20
$n_{\max}$	30
F	0.9
C	0.7
$\mathbf{L}$	$(0, 0.01, 0, 0.5, 0)$
$\mathbf{U}$	$(1, 0.5, 1, 1, 1)$

Figure 5 shows DE convergence by means of individual best per iteration (population) as well as an arithmetical average individual per nth iteration according to the following equation:

$$\bar{\mathbf{x}}^n = \frac{1}{N}\sum_{i=1}^{N}\mathbf{x}_i^n. \tag{30}$$

Quick convergence can be observed. Typically it takes five to ten iteration to reach the global optimum. The optimal Bézier curve, resulting in the lowest value of functional J, is shown in Fig. 6 which can be compared with other solutions in Fig. 2.

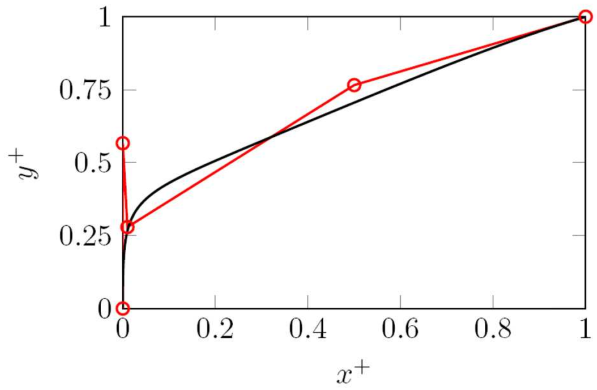

Figure 6: Optimal Bézier curve.

5 Summary

Two new approaches and solutions to minimum drag shape body problem have been introduced. Both transform the original variational problem to the classic problem of function optimisation. First approach is possible due to assumption of certain class of function, namely power law shapes. This makes it possible to find the optimal value of the exponent $n = 0.46$ being better than the classic $n = \frac{3}{4}$. Even better solution has been accomplished by means of a Bézier curve leading to discretised functional optimisation.
All solutions can be compared and ordered by means of the drag coefficient

$$c_d = \frac{R_x}{\frac{1}{2}\rho U_\infty^2 A}\ , \tag{31}$$

where $A = \pi y_0^2$ is the reference area. Table 2 presents the drag coefficient ratios where the reference drag, c_{dc}, has been calculated for cone. It is clear that the classic power law shape with the exponent $n = \frac{3}{4}$ is one of the worst. Modern global

Table 2: Drag coefficients ratios.

Curve	$\frac{c_d}{c_{dc}}$
$y^+ = x^+$	1.000
$y^+ = (x^+)^{\frac{3}{4}}$	0.880
$y^+ = (x^+)^{\frac{1}{2}}$	0.805
$y^+ = (x^+)^{0.46}$	0.803
Bézier	0.769

optimisation methods such as DE can produce better solutions characterised by lower drag.

Received in March 2016

References

[1] Anderson J.D.: *Modern Compressible Flow: With Historical Perspective*. McGraw-Hill, New York 1990.

[2] Eggers A.J., Besnikoff M.M. Jr., Dennis D.H.: *Bodies of revolution having minimum drag at high supersonic airspeeds*. NACA Rep. 1306, 1957.

[3] Elsgolc L.D.: *Calculus of Variations*. Dover Publications, New York 2007.

[4] Epstein P.S.: *On the air resistance of projectiles*. Proc. Nat. Acad. Sci. USA, **17**(1931), 9, 532–547.

[5] Grodzovskii G.L.: *Bodies of revolution with minimal drag coefficient and low heat transfer at high supersonic speeds*. Fluid Dyn. **3**(1968), 5, 52–58.

[6] Michalewicz Z.: *Genetic Algorithms + Data Structures = Evolution Programs*. Springer Verlag, Berlin, Heidelberg, New York 1996.

[7] Newton I.: *Principa–Motte's Translation Revised*. Univer. California Press, 1946.

[8] Peckham D.H.: *Measurements of Pressure Distribution and Shock-Wave Shape on Power-Law Bodies at a Mach Number of 6.85*. Aeronautical Res. Co. Tech. Rep., C.P. 871, London 1967

[9] Storn R., Price K.: *Differential evolution – A simple and efficient heuristic for global optimization over continuous spaces*. J. Global Optim. **11**(1997), 4, 341–359.

[10] Tesch K.: *Fluid Mechanics*. Gdańsk University of Technology Press, Gdańsk 2008 (in Polish).